Lakes, R. S., Nakamura, S., Behiri, J. C. and Bonfield, W., "Fracture mechanics of bone with short cracks", *Journal of Biomechanics*, 23, 967-975 (1990).

J. C. Behiri, W. Bonfield*
S. Nakamura§
and R. S. Lakes+

* Department of Materials, Queen Mary College, London, E1 4NS, U.K.
§ A.T.&T. Bell Laboratories, Crawford Corner Road, Holmdel, NJ, U.S.A.
+ University of Wisconsin

Abstract
Tensile fracture experiments were performed upon specimens of wet mature bovine Haversian bone, with short, controlled notches. Stress concentration factors were found to be significantly less than values predicted using a maximum stress criterion in the theory of elasticity. Results were also modeled with the aid of linear elastic fracture mechanics. Agreement of experiment with theory was better in this case, however deviations were seen for short notches. Two mechanisms were evaluated for the behavior: plasticity near the crack tip, and effects of the Haversian microstructure, modelled by Cosserat elasticity, a generalized continuum theory. Plastic zone effects were found to be insignificant. Cosserat elasticity, by contrast, predicted stress concentration factors which better approximated observed values. To explore strain redistribution processes, further experiments were conducted upon notched specimens in torsion at small strain. They disclosed a strain redistribution effect consistent with Cosserat elasticity. These microelastic effects are attributed to the Haversian architecture of bone.

INTRODUCTION

The ultimate properties of a material such as bone are specified not only by strength measures such as the ultimate tensile strength and yield strength, but also by measures of toughness. An investigation of toughness is of particular importance in materials such as bone and synthetic composites, which exhibit comparatively little nonelastic deformation prior to failure. Studies of fracture toughness in bone have been performed by Bonfield and Datta (1976) and by Behiri and Bonfield (1980), in which controlled cracks were introduced in bone specimens of well defined geometry.

Living bone contains microcracks which originate as a result of fatigue microdamage consequent to repetitive loading of bone during locomotion and other activities (Carter, et al., 1981). The toughness characteristics of bone in the presence of such microcracks are consequently of interest. In the present investigation, fracture experiments have been performed on bone specimens with short, controlled notches. The notch sizes were comparable to the size of the Haversian architecture of the bone. Consequently, analytical procedures incorporating some of the internal degrees of freedom of the microstructure have been utilized in the interpretation of the results. To explore some of the structural mechanisms for the toughness of bone, further experiments were conducted in which the deformation around notches was examined by holographic interferometry.

EXPERIMENTAL METHODS

A tensile fracture mechanics study was conducted in which specimens were prepared following the procedures outlined by Bonfield and Datta (1976). Specimens were machined slowly from the mid-diaphyses of adult bovine tibiae into standard strips 18 mm wide for tension testing. Bone specimens were examined microscopically and only those which were completely remodelled into a Haversian structure were retained for testing. The long axis of each specimen was aligned with the long axis of the original tibia. A single edge notch of controlled length and radius of curvature was machined into each specimen. Notch lengths of 0.25 mm (four specimens), 0.34 mm (four specimens), 0.50 mm (five specimens), 0.75 mm (three specimens), 14 mm (three specimens), 15 mm (two specimens), and 16 mm (two specimens) were used in this study. By contrast, the study of Bonfield and Datta involved specimens with relatively long notches 1.25 mm to 14 mm long. The specimens were stored in Ringer's solution at -20° C until testing. The specimens were loaded in tension until fracture, while saturated in Ringer's solution, in an Instron testing machine. The nominal strain rate was 3×10^{-4} s^{-1}. Fracture surfaces were then examined by scanning electron microscopy.

Experiments were also performed, in torsion, in which the deformation field around a notch was examined, for applied stress well below the yield point. The rationale was to ascertain whether processes responsible for toughening bone in the presence of stress raisers also operate in the regime of small stress. Yielding, for example, can effectively blunt a crack tip and increase the toughness, but the stress must be sufficiently high for yield to occur. For these experiments, a prismatic specimen of mature bovine Haversian bone was machined into a prism of square cross section 7.6 mm wide and 93 mm long. A small notch about 1 mm deep was made in the corner. The wet specimen was subjected to torsional load so that the maximum strain was 8×10^{-4} or less [well below the yield point] and the deformation field was evaluated by holographic interferometry (Lakes, et al., 1985). Briefly, this approach involves making a double exposure holographic interferogram using a single beam reflection technique ('piggyback holography'). The technique permits the experimenter to control the density of fringes in a selected region, in this case, near the notch. This experiment was repeated following air drying of the specimen. Interpretation of the results is based on the fact that the classical theory of elasticity predicts zero stress and zero strain at the corners of a twisted square cross section prism. There should therefore be no tendency for a notch at the corner to displace, hence any displacement found at the notch may be construed as evidence of nonclassical, eg., Cosserat elastic behavior predicted analytically by Park and Lakes (1987).

RESULTS

Scanning electron micrographs of typical fracture surfaces are shown in Fig. 1. These micrographs display the Haversian architecture of mature bovine cortical bone. The dependence of nominal tensile fracture strength σ_{fr} upon notch length c is displayed in Fig. 2 in which the strength is plotted vs $c^{-1/2}$, both for the present results and those of Bonfield and Datta(1976) for specimens with longer cracks. Fig. 2 also shows theoretical curves based on the classical elastic Inglis formula for a blunt notch, as well as the classical linear elastic fracture mechanics (LEFM) result for a sharp notch. Observe that the Inglis formula, which in the present context entails a fracture criterion based on maximum stress at the notch tip, severely underestimates the strength of bone in the presence of a notch. The LEFM curve, based on energy considerations, is obtained by curve fitting of the analytical curve to the experimental data as described by Bonfield and Datta(1976). The empirical relationship is:

$$\sigma_{fr}(\text{in MPa}) = 2.2\ c(\text{in meters})^{-1/2} - 6.0.$$

This equation embodies a correction for the finite width of the strip; the correction becomes important for relatively long notches. Fig. 3 shows the results plotted in terms of stress concentration factor for fracture vs crack length divided by crack radius of curvature. Theoretical curves based on different constitutive assumptions for the bone material are given for comparison.

The torsion experiment at small strain resulted in the holographic fringe patterns shown in Fig. 4. Each fringe corresponds to an out of plane displacement of 0.316 μm. In the wet bone, the observed discontinuity in fringe order across the notch (shown by an arrow) implies a shearing motion across the notch. By contrast the same specimen when dried displays no discontinuity in fringe order and hence no shear deformation of the notch.

ANALYSIS OF FRACTURE STUDY

Overview

In the analysis, a choice is to be made concerning the *fracture criterion* and concerning the *constitutive equation* for the bone material. Two fracture criteria are considered in this article. These are: a maximum stress criterion and a linear elastic fracture mechanics criterion. The maximum stress criterion specifies that fracture occurs when the maximum tensile stress anywhere in the specimen equals the ultimate tensile strength of the bulk material. Calculation of the maximum stress involves both the length of the crack and the tip radius of curvature. The linear elastic fracture mechanics approach involves consideration of fracture energy; only the crack length is considered.

As for the constitutive behavior, bone may be considered as (i) an elastic material, (ii) a Cosserat elastic material, (iii) as an elastoplastic material, or (iv) not a material but a structure. Cosserat elasticity is a continuum theory which incorporates some of the internal degrees of freedom of structured materials (Eringen, 1968, Cowin, 1970). Recent experimental studies have shown that Haversian bone behaves as a Cosserat elastic solid (Yang and Lakes, 1981, 1982, Park and Lakes, 1986). As for the other possibilities, it is well known that bone exhibits yield and is highly structured. Each constitutive assumption is treated individually below, both assuming a sharp notch and a blunt notch. The actual notches were blunt.

Elastic material

Bone may be considered to be a linearly elastic material for which the constitutive equation in one dimension is $\sigma = E\varepsilon$, in which σ is the axial stress, ε is the strain and E is Young's modulus. In three dimensions, we have, for an isotropic material,

$$t_{kl} = \lambda \varepsilon_{rr} \delta_{kl} + (2G)\varepsilon_{kl}$$

in which t_{kl} is the stress tensor, ε_{kl} is the small strain tensor, and λ and G are the elastic constants; G is the shear modulus. Bone is elastically anisotropic; the effect of anisotropy in the geometry used here is to increase the predicted stress concentration. Inasmuch as the observed stress concentrations for fracture are substantially *less* than values predicted by isotropic classical elasticity, the complications of anisotropic analysis will be dispensed with.

If the notch is viewed as perfectly sharp, a curve based on linear elastic fracture mechanics may be fitted to the data as was done by Bonfield and Datta, (1976). The the fracture strength σ_{fr} of a specimen with an edge notch of length c is given in linear elastic fracture mechanics by $\sigma_{fr} = K_{1c}/Yc^{1/2}$. Y is a correction factor to account for the finite width of the specimen(Brown and Srawley, 1966). In the case of short notches, the experimental data deviate from such a curve, as seen in Fig. 2. Moreover, for short notches, the notch root radius cannot be neglected in comparison with the notch length. It may be therefore more appropriate to view the notch as having a nonzero root radius of curvature. The notch may be considered as half an ellipse and the Inglis formula $\sigma_{fr} = \sigma_{ult}/[1 + 2(c/r)^{1/2}]Y$ applied for an elliptic hole. Here, σ_{ult} is the ultimate tensile strength of an un-notched specimen, c is the notch length, and r is its radius of curvature.

Such a model underestimates the strength of bone in the presence of a notch by more than a factor of two, as seen in Fig. 2.

Elastoplastic materials

Materials which exhibit yielding are predicted to form plastic zones near the tip of a crack. The radius r_y of the plastic zone is given approximately by the Dugdale solution (Knott, 1973):

$$2r_y = \pi^2\sigma^2 c/8\sigma_y^2$$

in which σ is the nominal applied stress, σ_y is the yield stress, and c is the crack length. The influence of plastic deformation is to effectively blunt the crack. Consider c = 1 mm, σ = 64 MPa, σ_y = 100 MPa in the context of the present experiments, then r_y = 0.25 mm. This is less than the root radius of the notches machined in the specimens. The crack blunting effect of plastic deformation is therefore minimal in the present experiments.

Cosserat elastic material

Bone may be considered to be a linear Cosserat (micropolar) elastic material. The rationale is that (i) experimental evidence of Cosserat elasticity has been found in bone by Yang and Lakes(1981-82); (ii) the Cosserat theory predicts stress concentrations around holes (Eringen, 1968, Cowin, 1970; Kaloni and Ariman, 1967) and cracks (Ejike, 1969; Sternberg and Muki, 1967) to be less than values based on classical elasticity; and (iii) the theory includes some of the freedom associated with material microstructure in a continuum form from which predictions can be made. The constitutive equations are (Eringen, 1968), in the isotropic case, as follows.

$$t_{kl} = \lambda\varepsilon_{rr}\,\delta_{kl} + (2\mu + \kappa)\varepsilon_{kl} + \kappa\varepsilon_{klm}(r_m - \phi_m)$$
$$m_{kl} = \alpha\,\phi_{r,r}\,\delta_{kl} + \beta\phi_{k,l} + \gamma\phi_{l,k}$$

in which t_{kl} is the asymmetric force stress, m_{kl} is the couple stress, $\varepsilon_{kl} = (u_{k,l} + u_{l,k})/2$ is the small strain, u is the displacement, and e_{klm} is the permutation symbol. The microrotation ϕ in Cosserat elasticity is kinematically distinct from the macrorotation $r_k = (e_{klm}u_{m,l})/2$. In three dimensions, the isotropic Cosserat elastic solid requires six elastic constants λ, μ, α, β, γ, and κ for its description. These are (Eringen, 1968, Cowin, 1970): Young's modulus $E = (2\mu+\kappa)(3\lambda+2\mu+\kappa)/(2\lambda+2\mu+\kappa)$, shear modulus $G = (2\mu+\kappa)/2$, Poisson's ratio $\nu = \lambda/(2\lambda+2\mu+\kappa)$, characteristic length for torsion $l_t = [(\beta+\gamma)/(2\mu+\kappa)]^{1/2}$, characteristic length for bending $l_b = [\gamma/2(2\mu+\kappa)]^{1/2}$, coupling number $N = [\kappa/2(\mu+\kappa)]^{1/2}$, and polar ratio $\Psi = (\beta+\gamma)/(\alpha+\beta+\gamma)$. When α, β, γ, κ vanish the solid becomes classically elastic.

In a sharp crack model, the Cosserat analytical solution (Sternberg and Muki, 1967) predicts a modest reduction in stress intensity at the crack tip, hence a corresponding increase in strength, for short cracks of length approaching the Cosserat characteristic length. The dotted curve shown in Fig. 2 was prepared under the assumption of a characteristic length of 0.2 mm (Lakes and Yang, 1983). The dependence of fracture stress upon notch length is modelled more accurately under the assumption of Cosserat elasticity than with classical elasticity, particularly for a short notch. The difference is, however, not large.

A blunt notch model is more appropriate in view of the experimental configuration used in this and earlier studies. For this model, some analytical results are available for elliptic holes in a Cosserat elastic material (Itou, 1973, Kim and Eringen, 1973), but not for the narrow ellipses required to model a notch. In this study, therefore, a finite element analysis(Nakamura, et al., 1984; Nakamura and Lakes, 1988) is used to obtain theoretical values of the stress concentration factor for elliptic notches. Stress concentrations were computed for various Cosserat characteristic lengths, including zero, which is equivalent to classical elasticity. These results, with the experimental values, are shown in Fig. 3. The finite element results for classical elasticity are seen to coincide with the results of the corrected Inglis formula, which is an exact solution. The predicted stress concentrations for Cosserat elasticity are substantially smaller than those for classical elasticity. The reduction in stress concentration depends on the Cosserat characteristic length. Characteristic lengths of 0.2 mm for torsion and 0.45 mm for bending have been measured for bone(Lakes and Yang, 1983), however owing to the anisotropy of bone, other characteristic lengths may be operative in the tensile fracture experiments.

INTERPRETATION OF TORSION EXPERIMENT

In the torsion of a notched bar of bone, motion was observed at the corner of the cross section, where classically it is predicted there should be neither stress nor strain. Thsi observation is in agreement with the results of Park and Lakes (1985) who reported strain distributions measured using micro strain gages in similar prismatic bars of human Haversian bone. These distributions were, in wet bone, in quantitative agreement with the predictions of Cosserat elasticity based on the torsional characteristic length reported earlier. By comparison with classical theory, the strian was redistributed in such a way as to reduce the peak strain and to increase the strain in regions [the corners] where classically it should be small. The interpretation of these results in the context of fracture mechanics is that wet bone can redistribute strain in inhomogeneous fields in a way favorable to the toughness. The redistribution mechanism is operative at small strain and requires the bone to be wet.

DISCUSSION

In the evaluation of materials, either the continuum view or the structural view may be taken. The continuum view is useful for making predictions and is essential in engineering applications. In this view, the complex structure of real materials is ignored and material properties derived from laboratory tests are used to predict the behavior of the material in other configurations. The structural view, by contrast, is more useful for understanding the causal mechanisms for the material behavior. In a highly complex material such as bone, the structural view is not suitable for the prediction of fracture. Structural arguments were invoked by Bonfield (1987) to explain the fact that changes in the crack tip radius of curvature had no influence on the fracture stress(Bonfield and Datta, 1976; Moyle and Gavens, 1986), contrary to the predictions of linear elastic fracture mechanics. Specifically, it was suggested that the fracture propagated from a microscopic flaw at the periphery of the machined notch tip. Moreover, the experimental results were extrapolated to the fracture stress of an 'non-cracked' specimen to obtain the 'critical flaw size' of the intact specimen. A value of 340μm was obtained by Bonfield and Datta, and a value of 1.82 mm was obtained by Moyle and Gavens. It is nonetheless remarkable that short notches produced virtually no concentration of stress and that the crack always started from the notch tip. In the continuum view, the significance of fracture mechanics results is, as pointed out by Bonfield (1987), that different crack lengths are associated with different fracture stresses, but with a common fracture toughness. The present results suggest that greater predictive power can be achieved by use of a generalized continuum model. As for the underlying causal mechanisms for the phenomena reported here, the compliant and weak interfaces in the Haversian structure are likely candidates. Nonetheless, there remain subtleties in the interpretation of fracture mechanics in bone as opposed to other materials which require further clarification (Bonfield, 1987).

CONCLUSIONS

1. Bone in the presence of a notch is tougher than expected on the basis of the theory of elasticity.
2. The toughness of bone cannot be accounted for in terms of plastic zone effects.
3. Strain is redistributed away from high strain regions to low strain regions. The effect occurs at small strain and is not dependent on yielding. The effect occurs in wet bone but not in dry bone.
4. Cosserat elasticity theory can account for much of the additional toughness of bone and for the strain redistribution phenomenon.

REFERENCES

Behiri, J. C. and Bonfield, W.(1980) Crack velocity dependence of longitudinal fracture in bone,*J.Materials Science*, **15,** 1841-1849.

Bonfield, W. (1987) Advances in the fracture mechanics of cortical bone, *J. Biomechanics***20**,1071-108.

Bonfield, W. and Datta, P. K. (1976) Fracture toughness of compact bone, *J. Biomechanics*, **9,**131-134.

Brown, W. and Srawley, J. (1966) Plane strain crack testing of high strength metallic materials, ASTM Publication 410, Philadelphia.

Carter, D.R., Caler, W.E., Spengler, D.M., and Frankel, V.H. (1981) Fatigue behavior of adult cortical bone: the influence of mean strain and strain range, *Acta Orthop. Scand.* **52**, 481-490.

Cowin, S. C. (1970) An incorrect inequality in micropolar elasticity theory, *J. Appl. Math. Phys.(ZAMP)* **21,** 494-497.

Currey, J. D. (1979) Changes in the impact energy absorption of bone with age, *J. Biomechanics,* **12,** 459-469.

Ejike, U.B.C.O. (1969) The plane circular crack problem in the linearized couple-stress theory, *Int. J. Engng. Sci.* **7,** 947-961.

Eringen, A.C. (1968) Theory of micropolar elasticity. In Fracture Vol. 1, 621-729 ed. by H.Liebowitz), Academic Press.

Itou, S.,(1973) The effect of couple-stresses on the stress concentration around an elliptic hole, *Acta Mechanica*, **16,** 289-296.

Kaloni, P. N. and Ariman, T. (1967) Stress concentration in micropolar elasticity, *J. Applied Mathematics, Physics (ZAMP)* **18,** 136-141.

Kim, B. S. and Eringen, A. C. (1973) Stress distribution around an elliptic hole in an infinite micropolar elastic plate, *Letters in Applied and Engineering Sciences*, **1,** 381-390.

Knott, J. F. (1973) Fundamentals of fracture mechanics, Butterworths, London.

Lakes, R. S., Gorman, D. and Bonfield, W. (1985) Holographic screening method for microelastic solids, *J. Materials Science* **20,** 2882-2888.

Lakes, R.S. and Yang, J.F.C. (1983) Micropolar elasticity in bone: rotation modulus κ, *Developments in Mechanics* **12,** 233-237

Moyle, D.D. and Gavens, A.J.(1986) Fracture properties of bovine tibial bone. *J. Biomechanics* **19**, 919-927.

Nakamura, S., Benedict, R. and Lakes, R. S. (1984) Finite element method for orthotropic micropolar elasticity, *Int. J. Engng. Sci.*, **22,** 319-330.

Nakamura, S. and Lakes, R.S. (1988) Stress concentration around a blunt crack in a Cosserat elastic solid, *Computer Methods in Applied Mechanics and Engineering,* **66**:257-266.

Park, H. C. and Lakes, R. S., (1986) Cosserat micromechanics of human bone: strain redistribution by a hydration sensitive constituent, *J. Biomechanics*, **19** 385-397.

Park, H. C. and Lakes, R. S., (1986) Torsion of a micropolar elastic prism of square cross section, *Int. J. Solids, Structures*, **23** 485-503.

Sternberg, E. and Muki, R. (1967) The effect of couple-stresses on the stress concentration around a crack, *Int. J. Solids, Structures*,**3,** 69-95.

Yang, J. F. C. and Lakes, R. S. (1982) Experimental study of micropolar and couple-stress elasticity in bone in bending, *J. Biomechanics*, **15,** 91-98.

Yang, J. F. C. and Lakes, R. S. (1981) Transient study of couple stress in compact bone: torsion, *J. Biomechanical Engineering*, **103** 275-279.

Figures

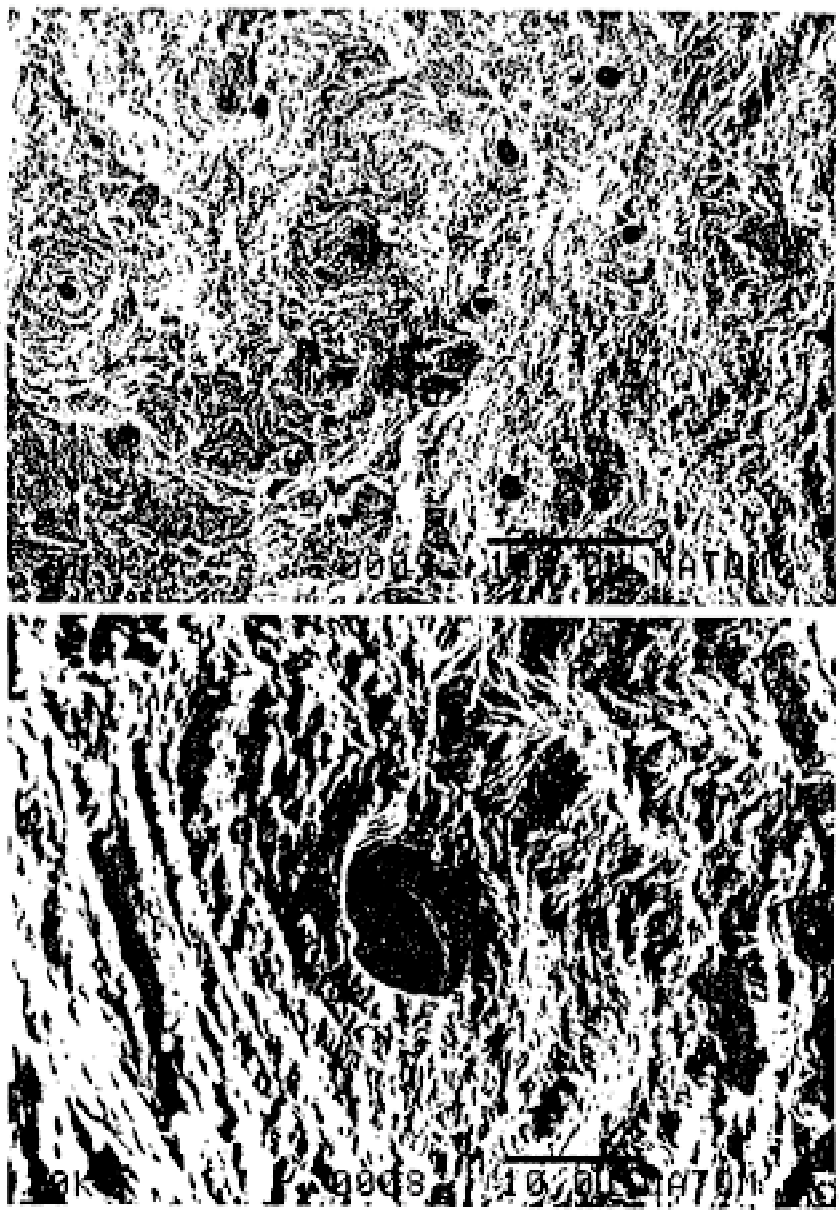

ig. 1. Scanning electron micrographs of fracture surfaces. Top, scale mark, 100 μm; bottom, scale mark, 10μm.

1. Scanning electron micrographs of fracture surfaces.
Top, scale mark, 100 μm; bottom, scale mark, 10 μm.

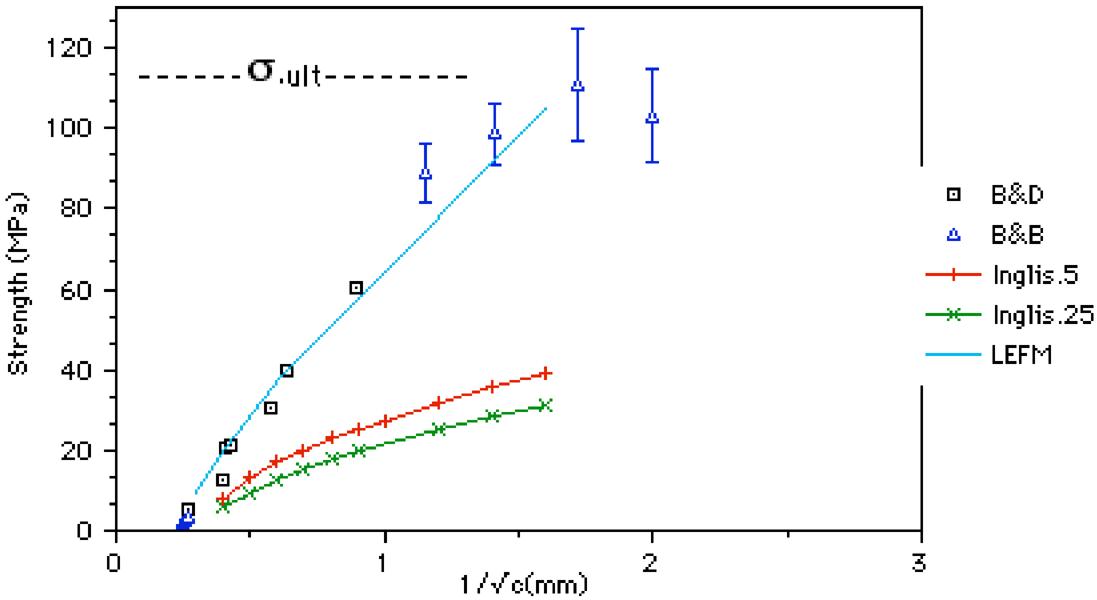

2. Nominal stress at fracture in tension vs 1/ √(notch length).
Û, squares: experimental results of Bonfield and Datta.
Δ, triangles: experimental results of present study.
Theoretical prediction of classical elasticity, maximum stress criterion:
+: Inglis formula for root radius 0.5 mm.
x: Inglis formula for root radius 0.25 mm.
Theoretical predictions of fracture mechanics models for assumed sharp crack:
Solid line: linear elastic fracture mechanics model.
Dotted line: Linear Cosserat elastic fracture mechanics model.
Both the fracture mechanics and Inglis formula curves have been corrected for the finite width of the specimen.

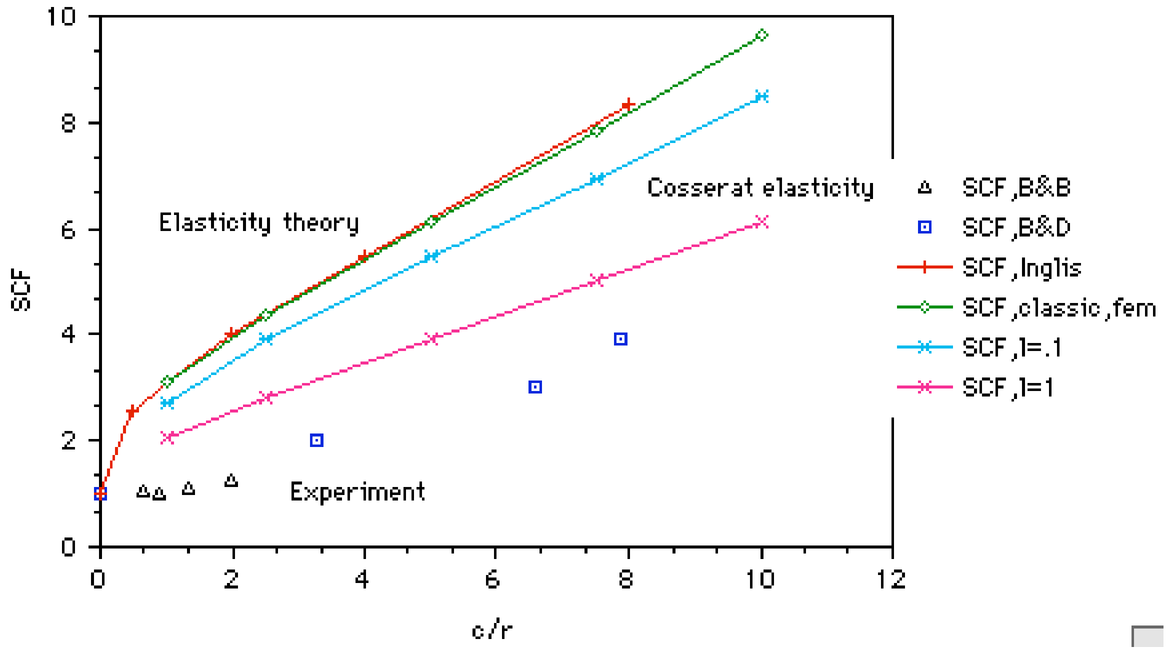

3. Stress concentration factor for fracture vs crack length/root radius.

Û, squares: experimental results of Bonfield and Datta(1976).

Δ, triangles: experimental results of present study.

Theoretical prediction of classical elasticity, maximum stress criterion, blunt crack:

+: Inglis formula.

◊, diamonds: Elasticity theory, finite element analysis.

x: Cosserat elasticity theory, finite element analysis, l = 0.1 mm, N = 0.93.

x-: Cosserat elasticity theory, finite element analysis, l = 1 mm, N = 0.93.

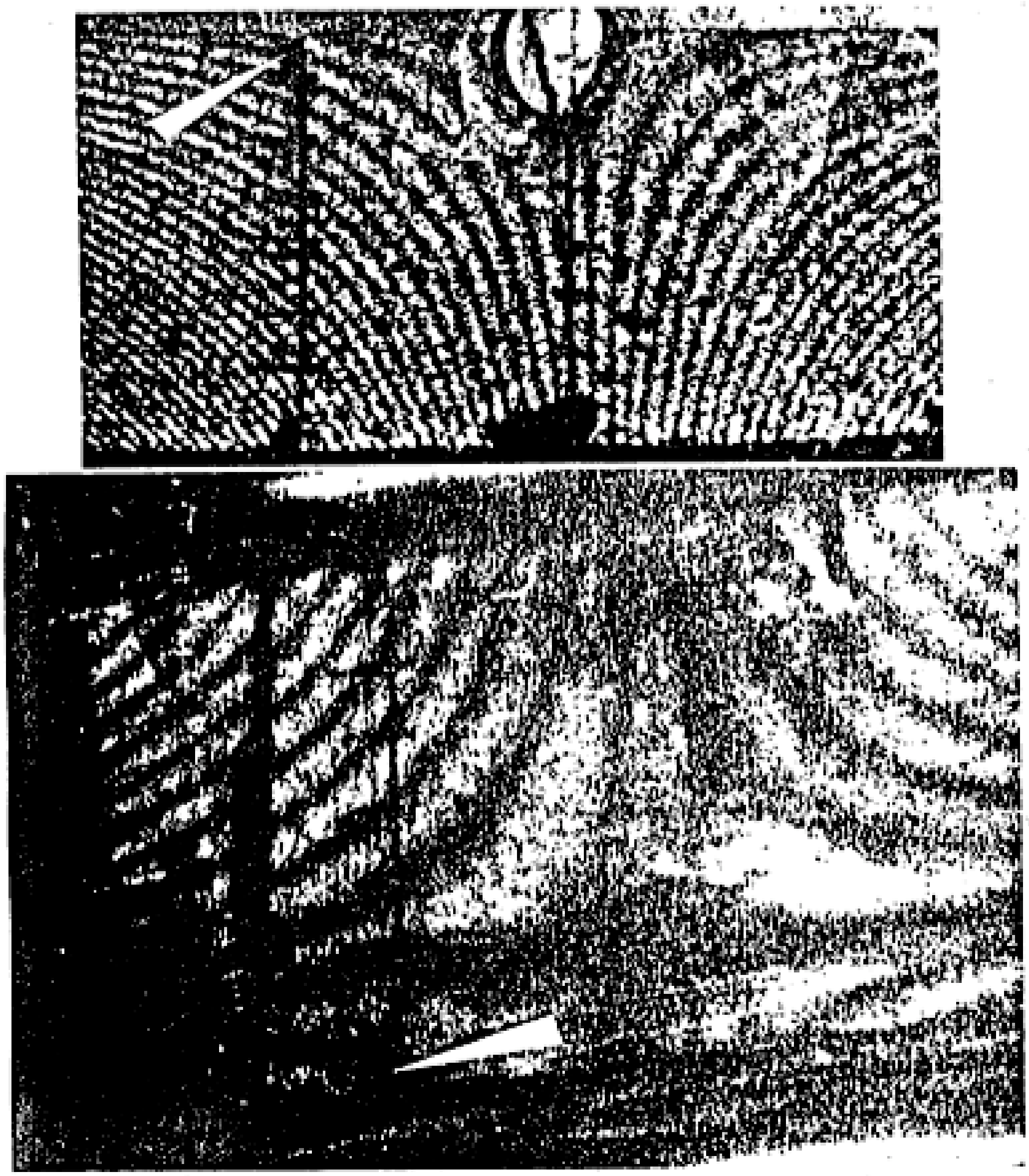

4. Holographic interferogram of prismatic bar in torsion. (a), top: dry bone; (b), bottom: wet bone.

Notch at corner of the cross section is shown by an arrow. The jump in fringe order at the notch in wet bone implies a shear motion.